TÜBİTAK

Turkish Journal of Earth Sciences

http://journals.tubitak.gov.tr/earth/

Research Article

Turkish J Earth Sci
(2021) 30: 973-989
© TÜBİTAK
doi:10.3906/yer-2104-3

Geology, mineralogy, and geochemistry of the Zarloukh Bentonite –Tuff deposit, Hemrin South Mountain, northern Iraq: implications for genesis and geotectonics

Yawooz A. KETTANAH*
Department of Earth and Environmental Sciences, Dalhousie University, Halifax, Canada

Received: 04.04.2021 • **Accepted/Published Online:** 06.11.2021 • **Final Version:** 22.11.2021

Abstract: The Quaternary Zarloukh Bentonite –Tuff (ZBT) deposit occurs within the Hemrin South Mountain, northern Iraq. The ZBT deposit occurs as depression-filling exposed on the erosional surface of the siliciclastic Pliocene Muqdadiya Formation and covered by an overburden of recent sediments. The thickness of the studied industrial bentonite bed is ~80–100 cm, occurring at the bottom of these depressions, covered by ~3–4 m thick bedded volcanic tuff, which also contains many 10–12 cm thick bentonite layers along its bedding planes. The volcanic ash at the bottom of lakes/swamps with shallow water content acted as basins for the deposition of falling volcanic ash, which immersed in water and devitrified to bentonite at a later stage by hydration and chemical interactions, meanwhile the continued fallen ash consolidated as tuff beds protecting the bentonite formed at the bottom of the depressions. The bentonite bed shows mini-scale trough crossbedding as a sign for its formation within a low energy, shallow agitated water in lakes/swamps. The bentonite and its precursor tuff show some differences in the concentration of Ca, Mg, Na, and K representing the exchangeable elements in smectite (montmorillonite), which is the predominant clay mineral in bentonite because of the probable gain of bentonite for these elements during the process of bentonitization of volcanic ash, which also formed the tuff. The ZBT has most probably the same origin as the Hemrin Basalt located NW of ZBT deposit. The chondrite-normalized REEs distribution pattern of ZBT and the Hemrin Basalt is similar, both showing enrichment and negative slope for the LREEs relative to the flat-lying HREEs. The Th vs. Co and the Th/Yb vs. Ta/Yb diagrams indicated that the ZBT and the Hemrin Basalt fall within the field of high-K calc-alkaline basalt and shoshonite and the andesitic basalt-andesite rocks reflecting their common origin.

Key words: Zarloukh deposit, bentonite, tuff, Hemrin basalt, montmorillonite, Iraq

1. Introduction

Bentonite is a commercial name for an industrial deposit consisting predominantly of montmorillonite with properties of swelling and water absorption. It has strong colloidal properties, and its volume increases several times when encountering water, creating a gelatinous and viscous substance. Bentonite deposits worldwide mostly originate from the hydrothermal or diagenetic alteration of pyroclastic rocks of intermediate to acidic compositions (e.g., Yalçin and Gümüşer, 2000; Abdioğlu and Arslan, 2005; Christidis and Huff, 2009; Arslan et al., 2010; Çiflikli et al., 2013; Modabberi et al., 2019; Kadir et al., 2021). Bentonite deposits occur in many countries including the USA, Germany, Greece, Spain, Italy, Algeria, Argentina, Australia, Italy, Japan, Hungary, Turkey, and Iran (Modabberi et al., 2019). Bentonite deposits are common in many parts of the neighboring Turkey (e.g., Çoban and Ece, 1999; Karakaş and Kadir, 2000; Yıldız and Kuşcu, 2004; Abdioğlu et al., 2004; Abdioğlu and Arslan, 2005; Yıldız and Kuşcu, 2007; Yıldız and Dumlupunar, 2009; Arslan et al., 2010; Karakaya et al., 2011; Kadir et al., 2011, 2021; Külah et al., 2017; Elliott et al., 2020). There are also many bentonite deposits in Iran (e.g., Fatahi et al., 2015, 2020; Khatami et al., 2012; Malek-Mahmoodi et al., 2013; Nakhaei et al., 2019; Modabberi et al., 2019). Unlike the currently studied surficial Quaternary Zarloukh bentonite deposit, all these Turkish and Iranian bentonites are older intraformational occurrences.

The studied ZBT deposit lies to the west of Hemrin Lake, some 180 kms to the south of Kirkuk City and about 18 kms east of the main road connecting the capital Baghdad with Kirkuk (Figures 1, 2). It is also about 16 kms to the southwest of another similar deposit called Qara-Tappa. The Qara-Tappa bentonite deposit was known for decades or possibly centuries, as it has previously been mined by hand drilled narrow tunnels and used by local people as hair softner. The Zarloukh bentonite was mined intermittently during 1960's to 1980's by open pit mining.

* Correspondence: kettanah@dal.ca

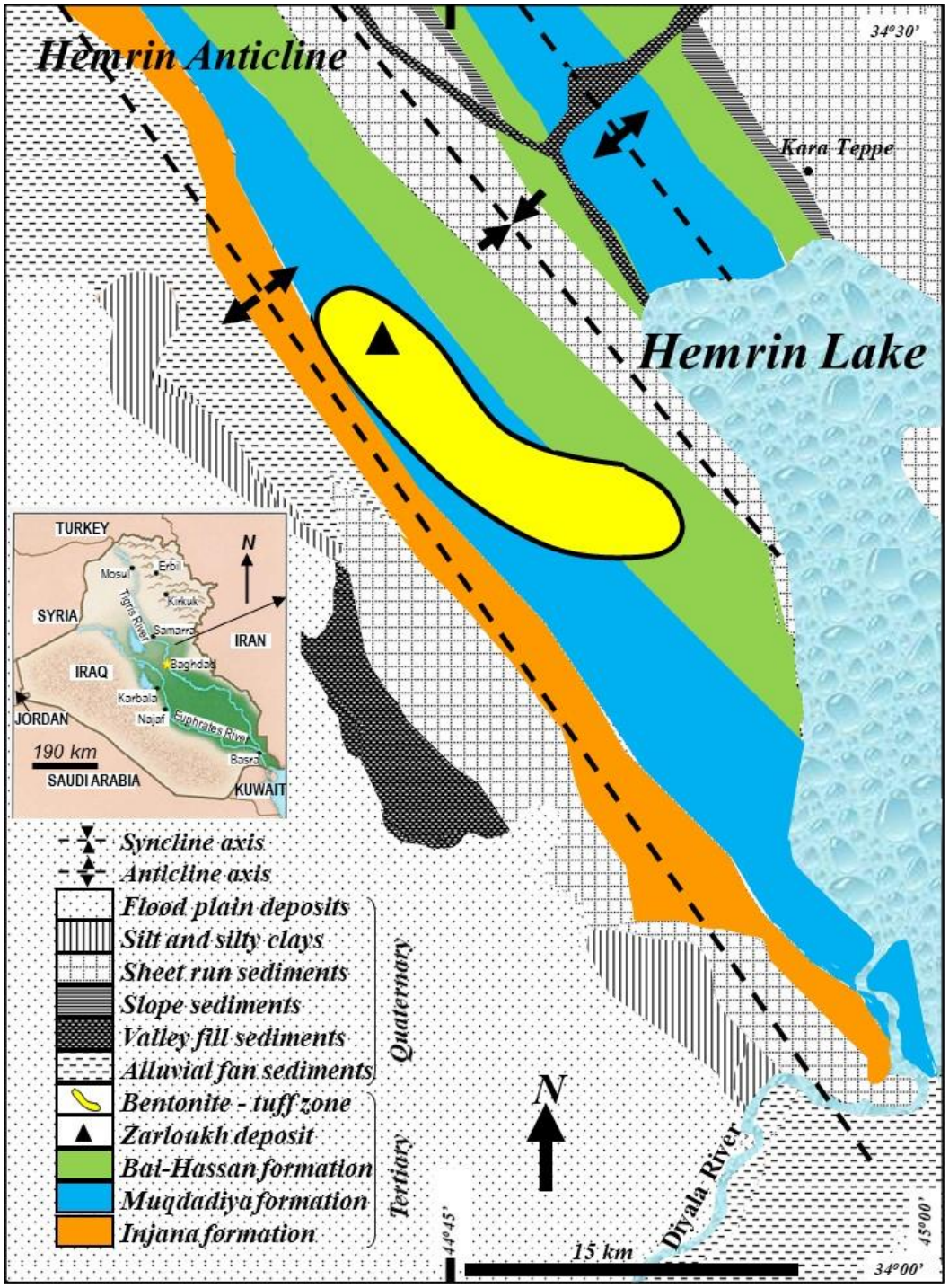

Figure 1. Geologic and location map of the study area showing the Zarloukh bentonite-tuff deposit.

Both the Qara-Tappa and Zarloukh bentonite deposits were scientifically reported for the first time by Zainal and Jargees (1972; 1973). Both deposits have many things in common including origin, geologic setting, and age, and together they form about 75% of the bentonite deposits in the region. These deposits occur as surficial depression fillings, mostly within the upper parts of the Muqdadiya (Lower Bakhtiyari) Formation as part of the Hemrin South Mountain range. Several other deposits were also reported by Al-Maini (1975) within the same formation in nearby areas such as Tayawi, Emgarin, and others, forming a zone of scattered and isolated small deposits (Figure 2a). A map

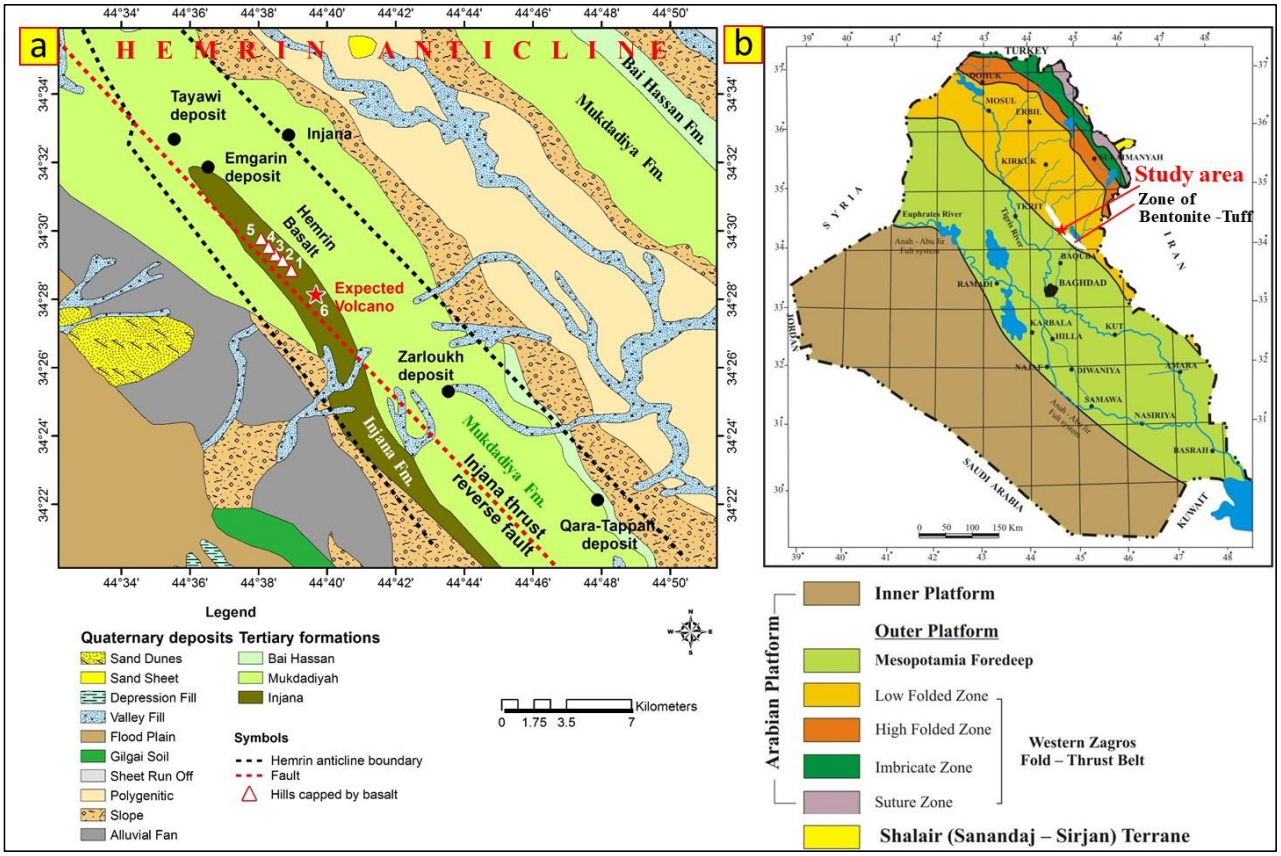

Figure 2. (a) Geologic map of the Hemrin South Mountain area (Barwary and Slewa, 2003) showing the locations of Zarloukh bentonite-tuff deposit and the other similar deposits as well as the hills (1 to 6) covered by the Hemrin Basalt, (b) Generalized tectonic map of Iraq showing the location of the study area (Sissakian and Fouad, 2012); the zone of bentonite-tuff is transferred from Al-Bassam (2012).

shown by Al-Bassam (2012) indicates that the bentonite-tuff deposits are scattered within a NW/SE trending zone of ~120 km length and ~10 km wide (Figure 2b). These bentonites are of Ca-montmorillonite type (Al-Bassam, 2012; Mohammed, 2019).

The tuff rocks of Zarloukh deposit are excellent insulator rocks because of their very light weight and high porosity, which can be used in its row state as building stone. However, the reserve of these rocks is not huge. The acid activated bentonites of Zarloukh and Qara-Tappa deposits were used in the purification of native sulfur at the Mishraq sulfur deposit, south of Mosul, Iraq (Mohammed, 2019). The estimated reserve of Zarloukh bentonite is about 300,000 tons (Zainal and Jargees, 1973); covering an area of ~0.3 Km^2 and extending for ~1400 m along a SE/NW direction (Al-Bassam, 2012). Many closely spaced depressions filled by bentonite-tuff beds were under open-pit mining operations during the field wok conducted during 1987–1988 for this study.

The aim of this study is to describe the characteristics and origin of bentonite and tuff of the Zarloukh deposit and to discuss its genetic relation and the other similar deposits in the area with the Hemrin Basalt within the Hemrin South Mountain, which was described by Kettanah et al. (2021).

2. Geologic setting

The ZBT deposit occupies many depressions within the upper part of Muqdadiya Formation (Pliocene). Tectonically, it is part of the Hemrin–Mekhul Subzone, which forms the lower part of the Low-Folded (Foothill) Zone of the unstable shelf of Iraq (Figure 2). The southern part of this tectonic zone is represented by the South Hemrin Fold, which constitutes the most prominent feature of the area. It is an asymmetrical anticline whose axis extends in the NW-SE direction (Figure 1). This anticline is part of a multifolded succession having similar trend, which are cut by many longitudinal and tranversal faults (Dunnington, 1958; Al-Naqib, 1967).

The Muqdadiya Formation was considered by van Bellen et al. (1959) as a group of fluviatile sediments filling depressions, derived from the high mountains of north and northeastern Iraq and adjacent areas; the age of which has been fixed as Pliocene due to the presence of Hipparion

fossils. It is made up of calcareous clays alternating with cross-bedded pebbly calcareous sandstones of various types and colors (Al-Naqib, 1960). The lower boundary of this formation with the Injana (Upper Fars) Formation is not sharp and marked by the first appearance of pebbly sandstone or a conglomerate bed. Meanwhile, its upper contact with the Bai-Hassan (Upper Bakhtiyari) Formation is marked by the first appearance of the coarse-grained conglomerate beds, which were eroded in many parts and, instead, occupied by Quaternary mixed river deposits. According to Kukal and Jassim (1971), the Muqdadiya Formation represents mollase sediments formed during the closing stages of the Zagros orogenic movement during Miocene-Pliocene period and deposited in fluviatile environments.

The studied ZBT deposit occurs as depression fillings, mostly within the upper parts of Muqdadiya Formation. The number of these depression-fillings is not known because of the overburden cover. They are sometimes very close to each other (almost connected), but, in other cases, few tens, hundreds or even kilometers apart. Their exposure dimensions are mostly few tens or hundreds of meters wide and few meters in depth. They have taken the shape of these depressions and are covered by flat lying, thickly bedded tuff beds. The bentonites within these depressions are white to very pale gray in color, in sharp contact with the hosting sandstone beds of Muqdadiya Formation. The underlying Muqdadiya Formation consists of greenish-grey, coarse-grained calcareous sandstones. The bentonite beds exist in the form of alternating layers with tuff beds (Figure 3). The main mined industrial bentonite bed is about 0.8 to 1 m thick and occupies the lower part of these depressions resting over the sandstones of Muqdadiya Formation. Meanwhile, the other 10–12 cm thick beds of bentonite occur at the bedding/joint planes within tuff beds. These layers have the same appearance and characteristics of the main industrial bentonite bed. The tuff beds have acted as ceiling and protecting cover of the bentonite deposits. Once the bentonite is exposed, these clays are very wet due to high water content and dark brown and greasy in feeling, and they start within seconds to crack and crumble into pieces and turn into a pale grayish white colored material due to instant loss of its water content by evaporation, a phenomenon that explains their absence directly on the surface without cover. The other significant feature of these bentonites is their fine, small-scale trough type cross bedding structures, containing within its laminae organic matters and fine-grained heavy minerals (Figure 4b). The individual cross-bedded structures are only few centimeters in dimensions.

The tuff beds overlying the bentonites are flat lying and thickly bedded (30–110 m in thickness). Both, the tuff and the bentonite beds are cut by three-directional perpendicular joints, and perhaps what looks like bedding planes within tuffs, coinciding with the horizontal joint planes. The steep dipping joints and fractures are filled by recent organic material. The tuffs are fine grained, homogeneous, well sorted, very light pink in color, and blocky but very light in weight. These layers have the same appearance and characteristics of the main industrial bentonite bed.

3. Sampling and methodology

Two sections named X and Z from two opposite parts of the main mined bentonite deposit were systematically sampled. The depression, which hosts the bentonite layers and the associated tuff beds, are ~4.5 m deep, and the bedding was flat. Eighteen samples from section X and twenty-six samples from section Z were collected to include some tiny lenses and thin layers of bentonite between the tuff beds (Figure 3). Up to five layers of bentonite bounded by tuff beds were observed in the studied open pit; they were named in this study from bottom to top as bed A, B, C, D and E, respectively. The last Surficial bed E is topographically at the same level with the local terrain of the area and mostly eroded, meanwhile the bottom A layer is the thickest and the main industrial part of the deposit (Figure 4). There are no observable changes in the thickness and properties of the bentonite and associated ceiling tuff throughout the studied mined deposit.

Different techniques and equipments were used in studying and analyzing the samples including X-ray diffraction (XRD), polarizing microscope, scanning electron microscope (SEM), neutron activation analysis (NAA), atomic absorption spectrometry (AAS), colorimetry, and wet chemical analysis. The Iraqi Nuclear Research Reactor was used for neutron activation analysis of major, trace and rare earth elements (Fe_2O_3, Na_2O, CaO, MgO, K_2O, TiO_2, Sc, V, Cr, Co, Rb, Zr, Hf, Ta, Th, U, La, Ce, Nd, Sm, Eu, Tb, Dy, Yb and Lu). The laboratories of the General Establishment of Geological Survey and Mining (Iraq) were used in analyzing major elements using wet chemical analysis for SiO_2, Al_2O_3, CaO and LOI, atomic absorption spectrometry (Pye-Unicam SP 2900) for Fe_2O_3, Na_2O, MgO, and K_2O, auto-analyzer colorimetry for TiO_2 and P_2O_5. PW 1965/60 Philips X-ray diffraction at the Department of Earth Sciences-Baghdad University (Iraq) and the scanning electron microscope of the Iraqi national oil company were used in mineralogical analysis. Details of these analytical procedures as well as precision, accuracy and sensitivity of the adopted methods using USA and Canadian international standards are given in El-Khafaji (1989).

The clay minerals were separated using wet sieving (Carver, 1971) followed by pipette analysis to separate clay fractions (<2μm) (Folk, 1974). Oriented slides

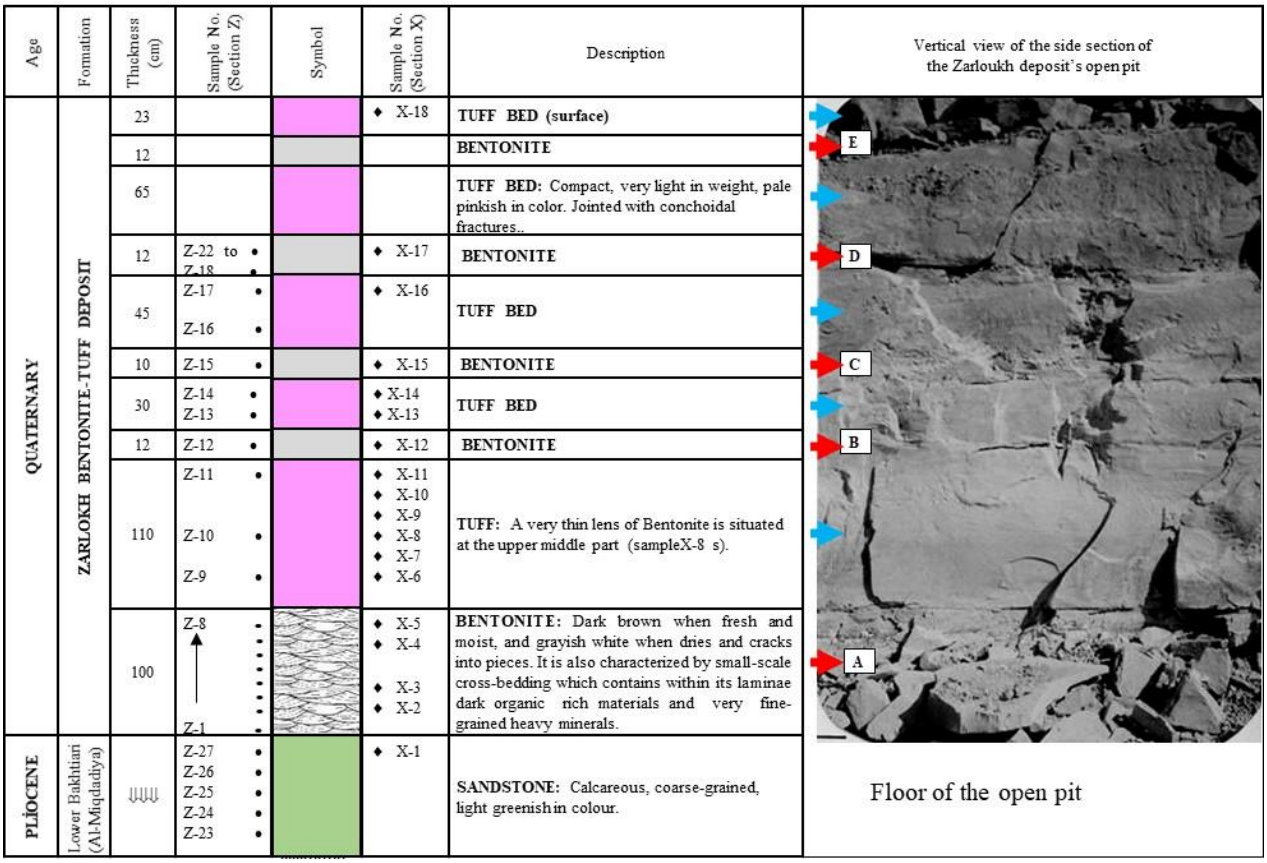

Figure 3. Field views and columnar section through the open pit of the Zarloukh Bentonite-Tuff deposit. X and Z represents the samples taken from two sections across the Zarloukh deposit on two opposite sides of the open pit.

were prepared using Carroll (1970) and Gipson (1966) methods for each sample. One slide was kept untreated, one ethylene glycolated, and the other two were heated to 350 °C and 550 °C, respectively using standard procedures (Brown, 1961). Relative abundance of clay minerals was semiquantitaivly calculated using the method of Carver (1971). Heavy minerals were separated using bromoform heavy liquid.

4. Results

4.1. Mineralogy

X-ray analysis of whole-rock bentonite samples showed that montmorillonite is the predominant clay mineral, while traces of quartz, dolomite ± gypsum are the associated minor nonclay minerals in these rocks (Figure 5a). Montmorillonite is the only clay mineral in the main industrial bentonite bed-A, which form the lower most bed of the deposit, meanwhile, minor amounts ranging from ~1 to 10% of illite and kaolinite appear in the thin bentonite layers within the bedding planes of tuff in the upper levels (Table-1; Figures 3, 5a, b-1 to b-3). The degree of crystallinity of montmorillonite was determined using Thorez (1976) and Biscaye (1965) methods, which showed that it is of good crystallinity with V/P index of 0.83 (Figures 5b-4). The tuff rocks consist dominantly of volcanic glass (~85%) and pyrogenic organic material (~15%) (Al-Hassan and Al-Zaidi, 2012).

Heavy mineral analysis and microscopic observations performed on both the bentonite and tuff indicated that bentonite contains bipyramidal zircon, biotite, and opaques, meanwhile the tuff contains euhedral zircon, hornblende, biotite, apatite, augite, and opaques; these minerals are associated with quartz and volcanic glass shards of tubular and lath-shaped appearance.

Scanning electron microscopic studies of bentonite and tuff showed honeycomb-like shaped montmorillonite clusters grown in hollows, bubble-shaped globules of the original tuffaceous material through which sporadic spheres of glass shards can be seen (Figures from 6-1 to 6-3). Views from tuff samples show various stages of devitrification and montmorillonite formation indicating genetic relation between the bentonite and tuff (Figures 6-1 to 6-3).

4.2. Geochemistry

The chemical analysis results for Zarloukh bentonite showed that it contains (as averages) 60.03% SiO_2, 14.28%

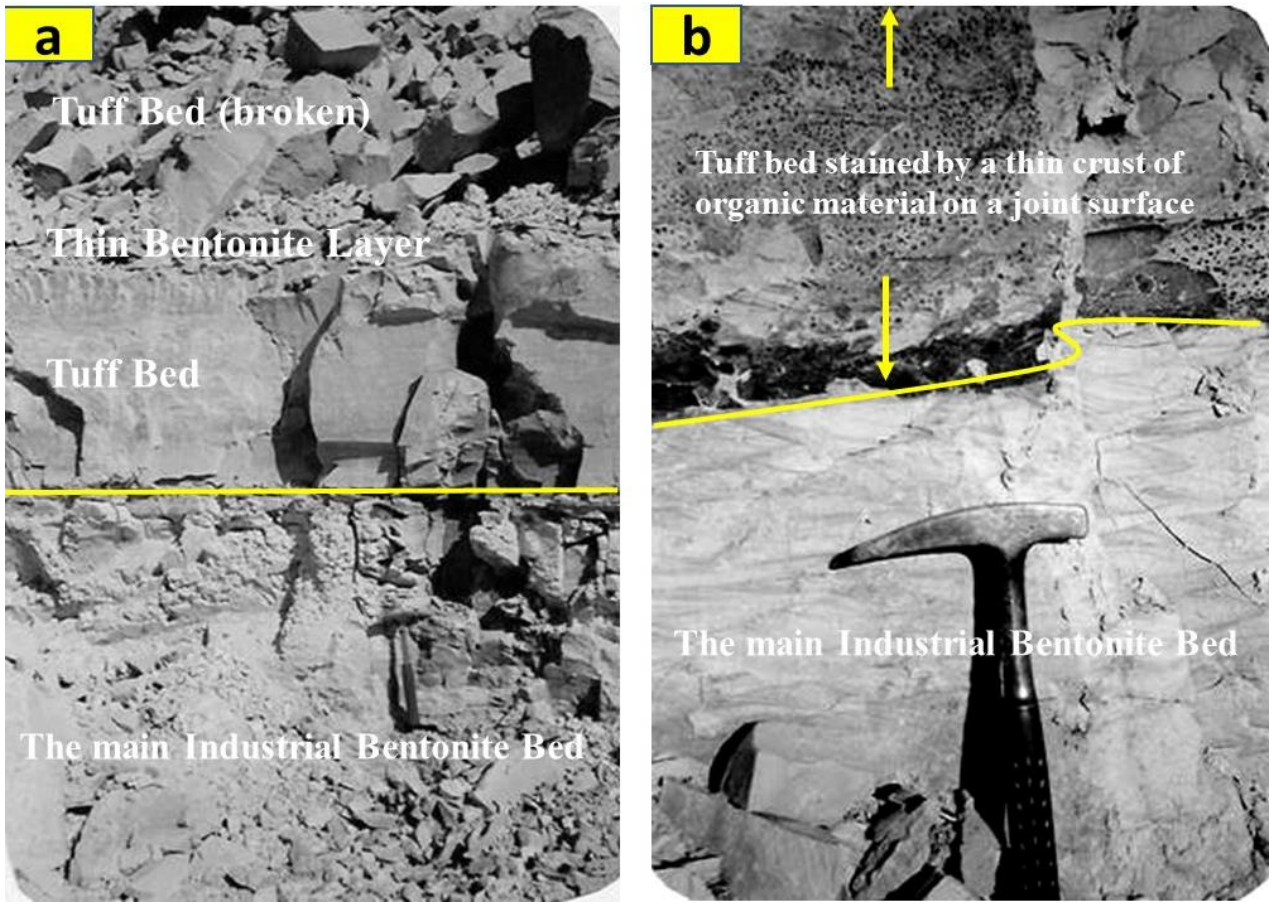

Figure 4. Field views of the bentonite and ceiling tuff beds: (a) Section X showing the main industrial bentonite bed at the bottom and the part of the covering thick tuff bed containing a thin horizon of bentonite, (b) Section Z showing small-scale cross bedding in the bentonite and a vertical joint plane in the tuff bed, which is stained by dark-colored spots and lumps of organic material (algae and fungi).

Al_2O_3, 1.81% Fe_2O_{3t}, 0.34% TiO_2, 2.46% CaO, 6.21% MgO, 0.82% Na_2O, 0.82% K_2O, 0.13% P_2O_5, and 9.28% LOI (Table 2; Figure 7a). Partial analysis for Zarloukh tuff showed that it contains 2.18% Fe_2O_{3t}, 0.34% TiO_2, 6.08% CaO, 8.41% MgO, 0.83% Na_2O, and 1.68% K_2O. This indicates that the bentonite and tuff show differences in the concentrations of many major elements such as Ca, Mg, Na, and K which are expected because the bentonite gains these elements as a result of the process of transformation of volcanic ash in the lower parts of the shallow water-bearing depressions (lakes/swamps) and its survival as tuff in the upper parts, which acted as capping rocks for the produced bentonite. For the same reasons, the bentonite and tuff show some minor differences in their average concentrations for some trace elements such as Sc, V, Rb, Zr, Hf, Th, Ta, La, and Ce, and very close and comparable values for other trace elements such as Co, Cr, U, and most of the analyzed REEs (Figures 7a, 7b; Table 2). The ΣREE content of bentonite and tuff is 146 ppm and 99 ppm, respectively. The ΣLREE relative to ΣHREE is enriched 20 and 34 times in bentonite and tuff, respectively. The chondrite-normalized REEs (Taylor and McLennan, 1985) distribution patterns are similar for the Zarloukh bentonite and tuff, and the Hemrin Basalt showing a negative slope and enrichment in LREEs relative to the nearly flat-lying HREEs (Figure 7b).

5. Discussion

The Zarloukh bentonite dominated by montmorillonite compared to its precursor tuff show expected differences in some key major element concentrations including Ca, Mg, Na, and K. Despite some differences in the average content of trace element values between bentonite and tuff, these differences are generally not very significant in most cases, suggesting the common origin of both (Figures 7a, b). Most of the unpublished reports on the bentonites of the Hemrin area, including the studied Zarloukh bentonite, have pointed to the derivation of bentonites

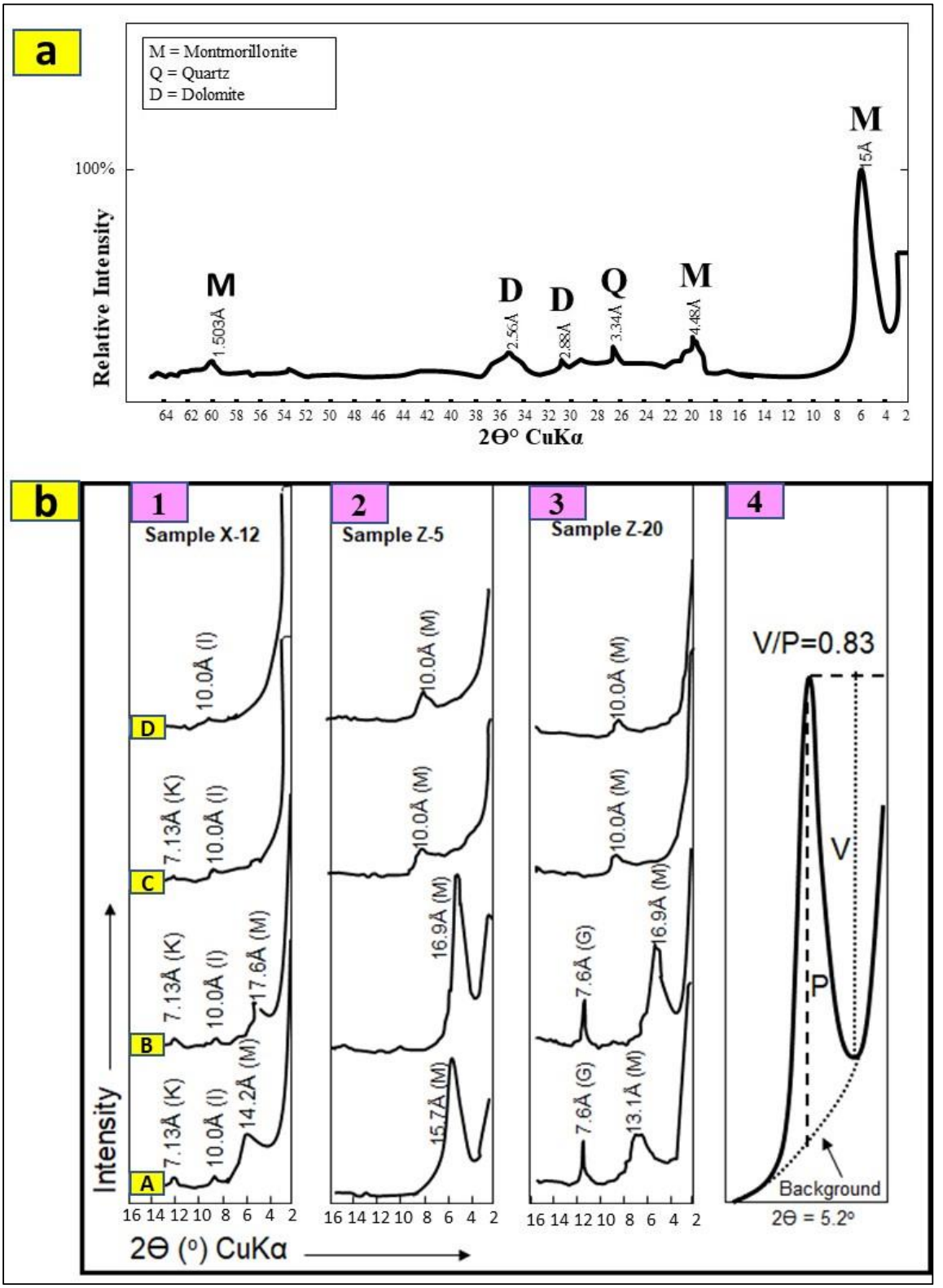

Figure 5. (a) Typical x-ray diffraction pattern of the whole rock from the main industrial bed of Zarloukh Bentonite (redrawn from the original diffractogram), (b) XRD diffractograms for clay separates (<2μm) from representative bentonite samples. (A) Oriented air-dried, (B) Ethylene glycolated, (C) Heated to 350°C, (D) Heated to 550°C. P, peak height; V,"valley" depth; V/P, crystallinity ratio of <2μm, glycol-expanded montmorillonite; M, montmorillonite, K, kaolinite; I, illite.

Table 1. Semi-quantitative estimates of the relative clay minerals content in Zarloukh bentonite. The units are seen in Figure 3.

Sample No.	Unit	Clay Mineral %		
		Kaolinite	Illite	Montmorillonite
Z22	Unit (d)	2	0	98
Z21		>1	<1	98
Z19		<1	>1	99
Z18		0	0	100
Z15	Unit (c)	4	3	93
Z12	Unit (b)	7	3	90
Z8	Unit (a) Main Bed	0	0	100
Z7		0	0	100
Z6		0	0	100
Z5		0	0	100
Z4		0	0	100
Z3		0	0	100
Z2		0	0	100
Z1		0	0	100

from the associated volcanic tuff (e.g., Zainal and Jargees. 1972, 1973; Zainal, 1977; El-Khafaji, 1989). The results of these studies on bentonites were summarized by Al-Bassam (2012) showing a map for the area where these deposits and other showings were located, indicating a NW/SE trending zone, ~120 km long and ~10 km wide, within the Hemrin South Mountain; the Hemrin Basalt also falls within this zone (Figure 2b). These previous studies have not mentioned a definite source for these bentonite and tuff deposits, but rather vaguely suggested without prove that they were possibly originated from the volcanic ashes emanated from the volcanic activities in the ophiolite zone of NE Iraq and/or the surrounding areas in Turkey and Iran, neglecting the fact that these bentonite-tuff deposits are of Quaternary age indicated from their surficial nature without having a cover from the host rock formations, meanwhile the ophiolites of northern Iraq and the surrounding Iran and Turkey are Cretaceous events and are not related in any way to the studied rocks.

The same area of bentonite-tuff deposits within the Hemrin South Mountain range also hosts what was previously known as burnt hills by Basi (1973) and Basi and Jassim (1974) (Figure 2a). The materials capping six of these hills (numbered as hill–1 to –6) were misinterpreted and misnamed by Basi (1973) and Basi and Jassim (1974) who suggested that they have been formed by burning and melting of sedimentary rocks of the Injana Formation by a jet of burning gases, along a NW/SE trending line near the axis of the Hemrin Anticline and close to the Injana thrust reverse fault (Figure 2a). Recent studies of these so-called burnt hills proved that they are basaltic rocks and originated from a volcanic activity in the area, possibly from the hill–6, about 10 km to the northwest of ZBT deposit (Abdulrahman, 2016; Kettanah et al., 2021). These basaltic rocks capping the hills were named Hemrin Basalt by Kettanah et al. (2021) suggesting that the source of this basalt and the bentonite-tuff deposits is the same volcanic activity, which ejected volcanic ash in the area to be deposited as volcanic tuff and followed by a lava flow, which formed the Hemrin Basalt during the Quaternary period, less than 0.5 Ma ago.

The chemical results of bentonite and tuff as well as those of the Hemrin Basalt (from Kettanah et al., 2021) plotted on the Th vs. Co diagram (Hastie et al., 2007) showed that they all fall in the same field (Figure 8a). All three rock types have basaltic andesite–andesites affinity and fall within the high-K calc-alkaline basalts and shoshonite field. The bentonite samples are equally divided between the basaltic andesite–andesite and the more acidic group of volcanic rocks (dacite-rhyolite-latite-trachyte) zones, and one of them show basaltic affinity. The Th/Yb vs. Ta/Yb diagram (Pearce, 1983) also shows that the ZBT and the Hemrin Basalt fall in the medium- to high-K calc-alkaline basalt field (Figure 8b). These two diagrams clearly suggest the same origin for the Hemrin Basalt and the tuff and associated bentonite deposits of the studied Zarloukh area, which is also expected for the other similar bentonite-tuff deposits in the surroundings. This result is a further confirmation for the conclusion reached by Kettanah et al. (2021) about the common origin of these three rock types in the Hemrin area. Bentonite deposits of Balıkesir region, NW Turkey (Kadir et al., 2019) and few east Aegean islands and western Thrace region, NE Greece (Koutsopoulou et al., 2016) fall in the same field of

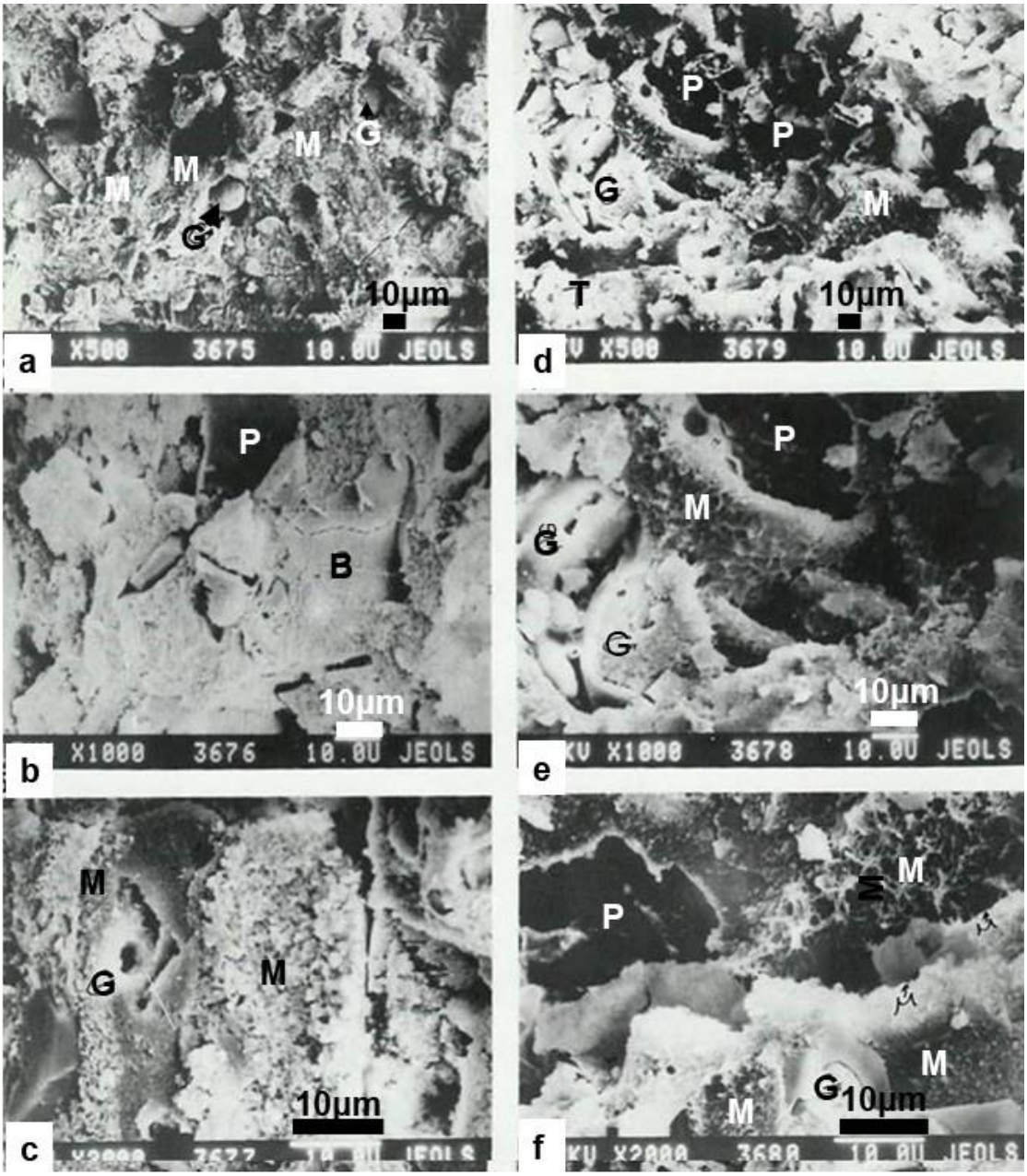

Figure 6. SEM views for a representative bentonite and tuff from Zarloukh Bentonite deposit showing globular and bubble-shaped aggregates of montmorillonite (1, 2, 3) and tuff (4, 5, 6) showing various stages of devitrification and formation of montmorillonite (M). Open spaces and pores (P) are evident within and between the globules. Few spheres of survived glassy material (G) are scattered between honeycomb like aggregates of montmorillonite.

the studied ZBT deposit in the Th vs. Co diagram of Hastie et al. (2007). The Th/Yb vs. Ta/Yb tectonic discrimination diagram (Wilson and Bianchini, 1999) showed that the Zarloukh bentonite and tuff and the Hemrin Basalt are of orogenic (collision-related) origin (Figure 9).

The currently studied bentonite-tuff deposit and the surrounding similar deposits in the area can be considered unique in their type because they are recent Quaternary occurrences formed at the eroded surface of the Muqdadiya Formation and has no genetic relation to their host formation unlike all bentonite occurrences in the neighboring Turkey and Iran; in the introduction, all those occurrences were mentioned as older intraformational deposits.

A schematic scenario for the possible mode of the formation of the Hemrin Basalt and the Zarloukh and

Table 2. Whole-rock geochemistry of the Zarloukh bentonite and tuff, and the Hemrin Basalt. The data for Hemrin Basalt are from Kettanah et al. (2021).

Rock type	Zarloukh Bentonite													
Sample No.	X-2	X-5	X-8	X-12	X-15	Z-1	Z-2	Z-3	Z-5	Z-6	Z-7	Z-8	Z-12	Z-15
Major oxides (%)														
SiO_2	60.76	59.50	–	62.03	–	–	–	–	60.85	–	–	62.50	64.80	49.80
Al_2O_3	14.62	14.60	–	14.34	–	–	–	–	15.47	–	–	14.34	13.40	13.20
Fe_2O_{3t}	1.78	2.31	1.87	2.76	3.51	1.99	2.11	2.07	0.78	0.84	0.60	2.25	3.30	3.30
TiO_2	0.30	0.35	0.52	0.38	0.69	0.06	0.07	0.07	0.30	0.61	0.11	0.25	0.30	0.39
CaO	2.80	2.80	1.30	2.52	ND	1.84	1.16	1.54	2.52	1.53	1.45	3.08	2.24	3.50
MgO	8.96	7.20	4.39	4.70	4.50	8.21	7.90	6.90	7.50	6.51	7.51	4.69	3.70	7.20
Na_2O	0.47	0.40	0.42	0.59	1.55	0.50	0.50	0.47	0.21	0.61	0.67	1.19	2.35	2.60
K_2O	0.51	0.59	0.72	1.55	0.72	0.72	0.16	0.72	0.35	0.72	0.59	0.96	1.80	1.23
P_2O_5	0.15	0.19	–	0.12	–	–	–	–	0.16	–	–	0.10	0.06	0.12
LOI	8.57	8.82	–	8.16	–	–	–	–	8.93	–	–	8.96	7.45	14.07
Trace elements (ppm)														
Sc	5.35	6.56	2.10	1.33	9.90	5.02	ND	4.80	2.90	3.90	4.04	2.90	0.97	6.12
Co	9.04	8.69	5.57	15.20	11.07	8.89	10.80	5.54	7.69	5.00	6.88	ND	10.00	6.35
Cr	97.57	106.80	13.25	33.93	67.87	64.15	38.00	54.55	27.63	27.50	48.20	24.60	23.34	64.00
V	–	–	125.40	103.36	–	101.30	98.40	88.90	107.90	111.50	61.40	18.00	63.80	61.70
Rb	38.40	26.60	112.50	93.10	118.70	30.60	18.80	ND	15.70	12.12	21.42	59.30	124.50	61.35
Zr	23.93	31.60	–	–	–	–	–	13.79	–	–	62.10	75.60	–	–
Hf	4.88	4.96	4.17	4.70	3.38	5.69	5.46	5.01	4.45	4.10	3.75	3.80	4.28	2.56
Th	32.01	31.99	28.10	27.20	20.99	37.34	36.30	35.10	28.40	32.20	28.28	25.30	27.60	15.80
U	3.24	3.07	3.90	3.74	4.50	4.00	4.60	4.01	3.50	3.80	3.90	2.20	6.40	2.32
Ta	1.25	1.23	0.94	1.06	0.92	2.92	1.35	1.22	0.91	1.69	1.37	1.21	1.02	0.75
Sb	0.46	0.78	0.78	–	0.72	0.44	–	–	–	0.53	0.79	–	0.39	0.39
Rare earth elements (ppm)														
La	60.50	55.30	40.90	35.90	47.00	65.90	48.50	56.90	34.72	53.60	53.90	36.30	40.70	36.12
Ce	76.71	69.67	68.50	56.50	62.03	81.24	89.00	70.89	69.64	59.59	62.15	41.50	37.09	46.96
Nd	20.97	19.26	13.50	11.90	16.79	18.34	16.79	16.51	14.90	15.13	14.70	13.69	13.26	14.90
Sm	4.51	7.95	0.42	2.31	6.08	4.06	6.91	3.85	5.80	9.57	5.50	0.54	6.07	0.82
Eu	0.53	0.78	0.63	0.88	0.85	0.57	1.13	0.52	0.93	0.85	2.13	0.50	1.06	0.75
Tb	0.56	0.57	0.23	0.23	0.64	0.48	0.31	0.39	0.23	0.51	0.44	0.44	0.27	0.44
Dy	–	–	–	–	–	–	–	–	5.81	–	–	1.01	3.43	–
Yb	1.69	2.71	1.27	3.50	2.63	2.26	2.60	2.00	2.99	2.86	2.80	1.80	2.80	1.80
Lu	0.51	0.53	0.11	0.10	0.56	0.57	0.55	0.56	0.62	0.41	0.42	0.28	0.44	0.36

Table 2. (Continued).

Rock type	Zarloukh Bentonite							Zarloukh Tuff			Hemrin Basalt		
Sample No.	Z-18	Z-19	Z-20	Z-22	Minimum	Maximum	Mean	X-16	Z-11	Mean	Minimum	Maximum	Mean
Major oxides (%													
SiO_2	–	–	–	–	49.80	64.80	60.03	–	–	–	49.86	55.70	52.68
Al_2O_3	–	–	–	–	13.20	15.47	14.28	–	–	–	11.57	14.48	13.21
Fe_2O_{3t}	1.01	0.73	0.97	0.40	0.40	3.51	1.81	2.25	2.10	2.18	4.93	7.60	6.20
TiO_2	0.45	0.69	0.26	0.29	0.06	0.69	0.34	0.49	0.19	0.34	0.67	0.77	0.72
CaO	1.59	1.54	2.48	7.90	1.16	7.90	2.46	6.26	5.90	6.08	9.95	14.97	13.55
MgO	4.80	5.12	6.15	5.90	3.70	8.96	6.21	8.50	8.32	8.41	3.01	6.28	4.56
Na_2O	0.46	0.56	0.54	0.65	0.21	2.60	0.82	0.95	0.70	0.83	1.70	2.16	1.94
K_2O	0.70	0.50	1.03	1.19	0.16	1.80	0.82	2.50	0.85	1.68	2.12	2.81	2.46
P_2O_5	–	–	–	–	0.06	0.19	0.13	–	–	–	0.13	0.19	0.17
LOI	–	–	–	–	7.45	14.07	9.28	–	–	–	1.28	6.51	4.05
Trace elements (ppm)													
Sc	5.57	1.50	5.37	8.00	0.97	9.90	4.49	1.24	3.60	2.40	12.00	18.00	14.83
Co	5.90	27.70	15.03	14.50	5.00	27.70	10.23	11.40	15.60	13.50	16.00	27.00	22.75
Cr	49.00	40.30	68.00	101.50	13.25	106.80	52.78	57.50	44.00	51.00	200.00	450.00	319.17
V	88.02	133.60	120.60	155.90	18.00	155.90	96.00	144.70	156.90	151.00	1013.00	7007.00	1931.92
Rb	–	29.03	32.90	47.60	12.12	124.50	52.69	84.60	139.60	112.50	66.00	99.00	84.83
Zr	68.25	–	424.00	–	13.79	424.00	99.86	50.00	–	50.00	134.00	163.00	146.17
Hf	4.45	5.18	5.46	4.60	2.56	5.69	4.49	3.45	3.37	3.45	2.20	3.50	3.17
Th	29.40	31.70	34.80	24.90	15.80	37.34	29.28	14.60	24.40	19.50	6.90	9.50	8.26
U	1.95	3.63	2.53	3.41	1.95	6.40	3.59	3.40	4.60	4.00	2.90	15.10	4.30
Ta	1.43	1.23	1.55	1.57	0.75	2.92	1.31	0.55	1.22	0.90	0.90	1.10	0.95
Sb	–	–	0.65	–	0.39	0.79	0.59	–	–	–	0.90	1.70	1.27
Rare earth elements (ppm)													
La	54.70	65.49	53.60	51.80	34.72	65.90	49.55	36.60	22.40	29.50	24.40	29.60	27.13
Ce	71.10	113.09	74.30	57.90	37.09	113.09	67.10	48.70	30.70	39.70	45.90	64.80	52.65
Nd	19.70	23.20	20.80	18.60	11.90	23.20	16.83	19.50	25.40	22.45	20.70	32.90	24.01
Sm	3.97	9.26	4.24	6.11	0.42	9.57	4.89	3.56	2.90	3.23	4.10	7.60	5.04
Eu	0.59	1.35	0.80	1.04	0.50	2.13	0.88	1.05	0.76	0.91	0.97	1.84	1.16
Tb	0.33	0.35	0.44	0.44	0.23	0.64	0.41	0.25	0.44	0.35	0.60	1.00	0.73
Dy	–	5.20	–	–	1.01	5.81	3.86	–	–	–	3.80	5.90	4.33
Yb	1.48	2.62	1.70	2.33	1.27	3.50	2.32	2.33	1.90	2.12	2.20	3.00	2.51
Lu	0.25	0.42	0.34	0.34	0.10	0.62	0.41	0.36	0.36	0.36	0.32	0.43	0.36

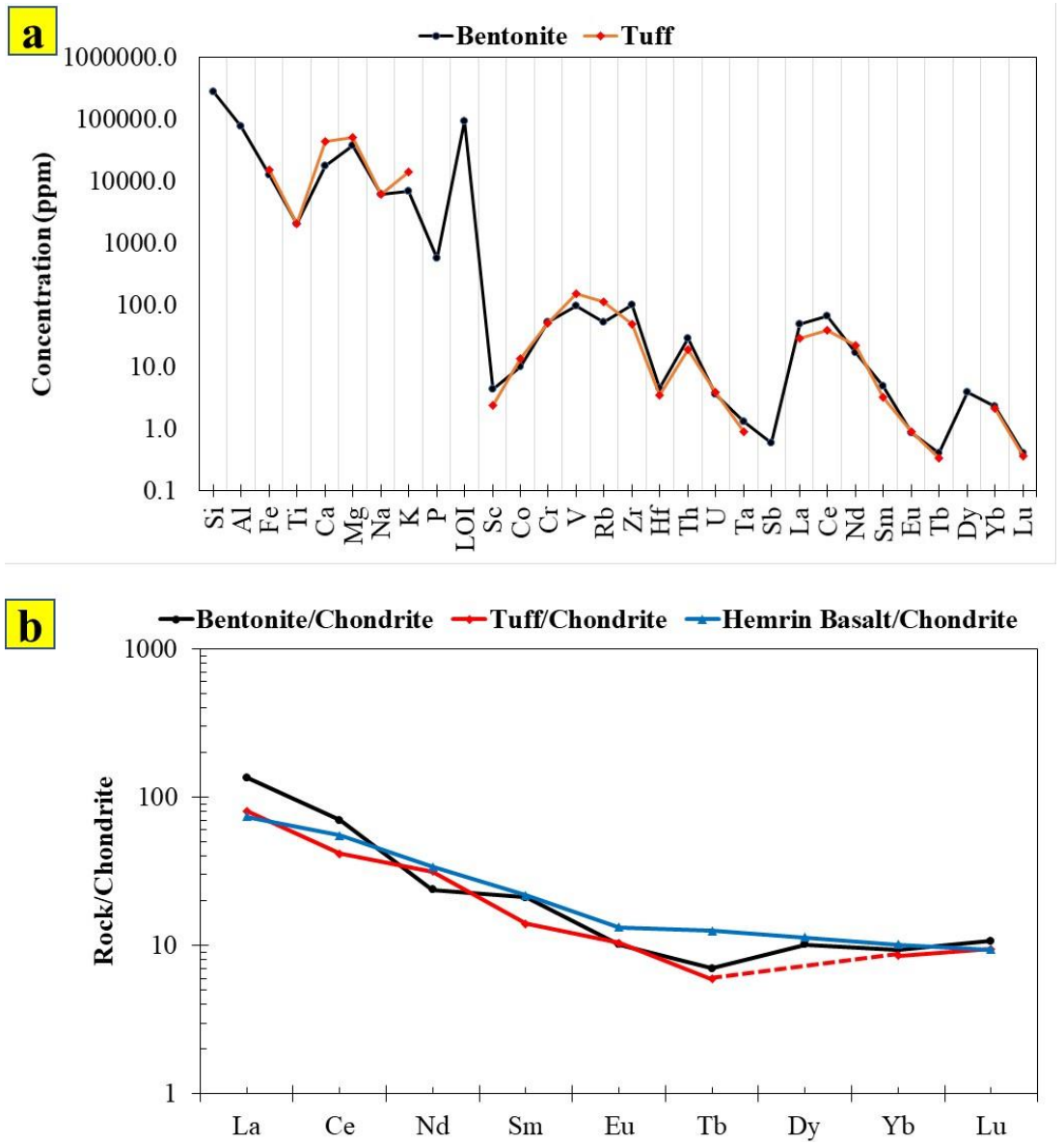

Figure 7. (a) Whole-rock geochemistry of bentonite and tuff, (b) Chondrite-normalized REE for the Zarloukh Bentonite and Tuff, and the Hemrin Basalt (Taylor and McLennan, 1985).

the other similar bentonite-tuff deposits in the study area within the Hemrin South Mountain is illustrated in Figure 10. Based on this scenario, the Zarloukh tuff was formed during Quaternary period by deposition of volcanic ash erupted from the Hemrin volcano over the Hemrin area, filling shallow water surficial depressions (lakes/swamps). The volcanic ash apparently covered the whole area, but the only survived parts are those deposited in the shallow lakes/swamps distributed in the region at that time. The first deposited ashes immersed in the shallow water content of these depressions to be converted later to smectite by hydration and chemical interactions to form bentonite, allowing the succeeding deposited ash to survive and lithify as tuff beds (Figures 3, 4). The proof of this is that the main industrial bed of bentonite (~1 m thick) rests directly on the sandstones of Muqdadiya Formation within these depressions and are covered by 3–4 m thick tuff beds (Figure 3). The first deposited ashes show micro-scale trough cross bedding, apparently produced by the gently agitated water in lakes/swamps during deposition (Figures 3, 4b). Such shallow water lakes and swamps exist even today in the area. Once the wet ash was covered by the succeeding dry ash, the process of transformation of the volcanic ash started by devitrification of the volcanic glass, hydration, and crystallization producing montmorillonite bentonite. The tuff and the bentonite show different

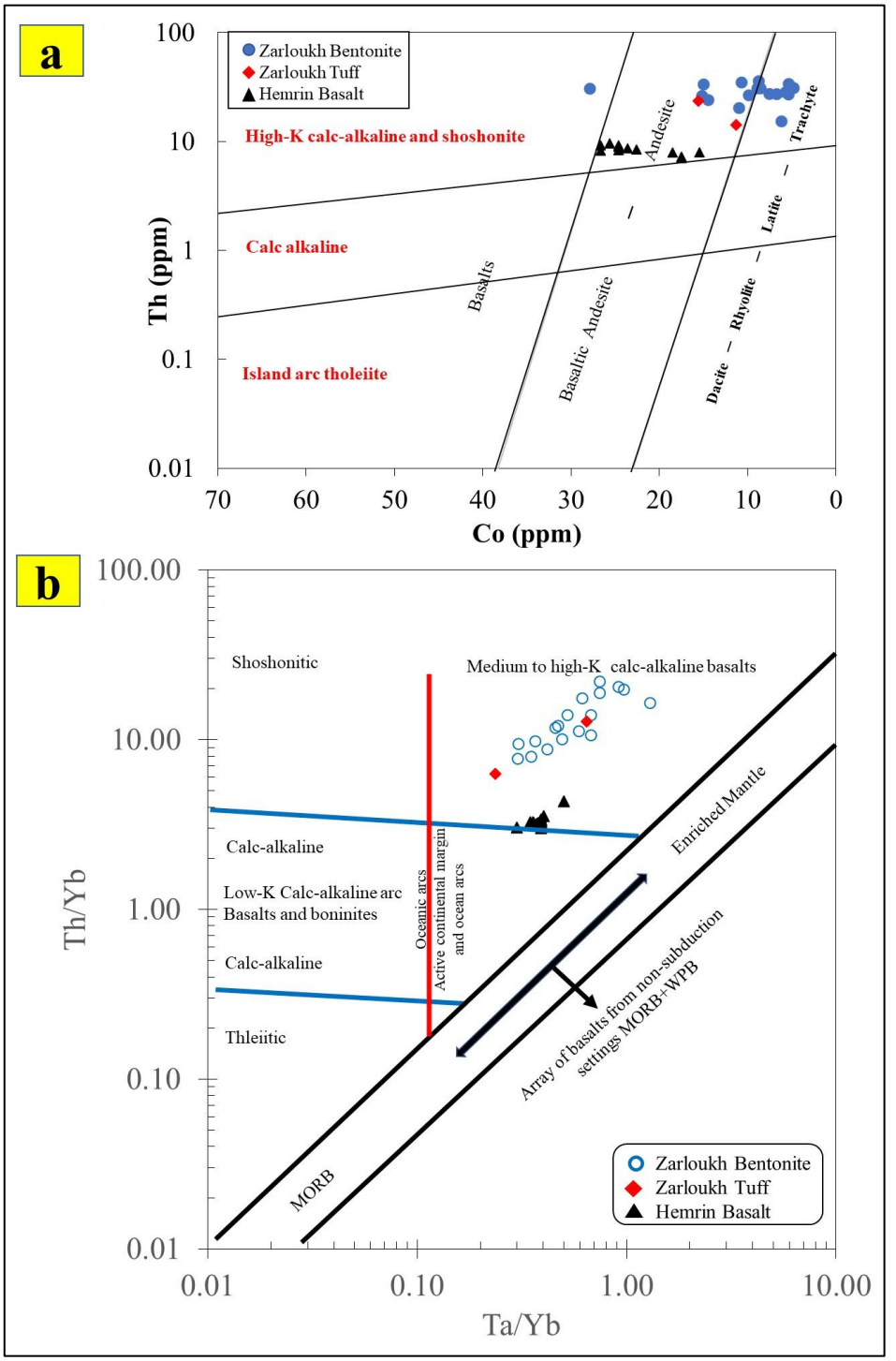

Figure 8. (a) Binary Co vs. Th discrimination plot (Hastie et al., 2007) for the Zarloukh Bentonite and tuff and the Hemrin Basalt, (b) Binary Th/Yb vs. Ta/Yb (Pearce, 1983). The data for Hemrin Basalt are from Kettanah et al. (2021).

average concentrations for some major elements such as Ca, Mg, Na, and K, which are the exchangeable elements in montmorillonite, reflects the process of transformation of the volcanic glass in tuff to montmorillonite in bentonite by devitrification with hydration and crystallization processes. The smectite mineral group generally form

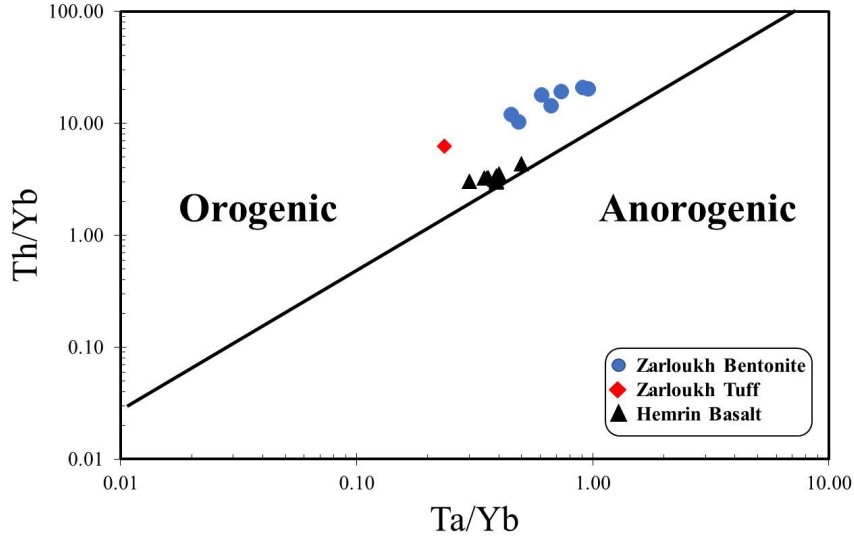

Figure 9. Th/Yb vs. Ta/Yb tectonic discrimination diagram (Wilson and Bianchini, 1999).

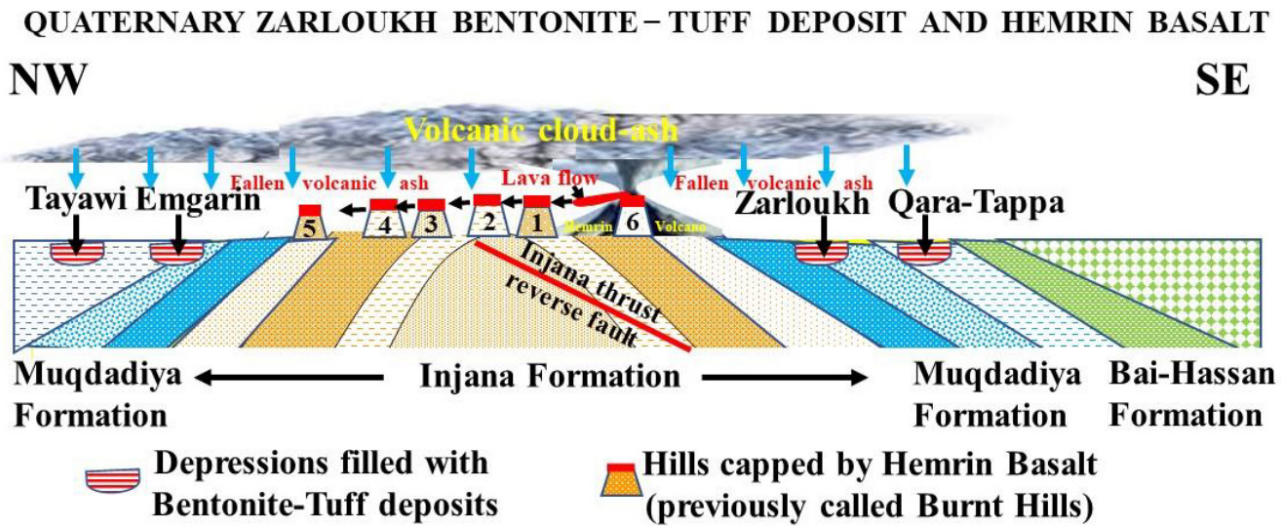

Figure 10. Schematic scenario for the possible formation of the Zarloukh bentonite and tuff and the Hemrin Basalt by the same volcano.

by chemical alteration of volcanic ash, tuff and lavas containing abundant volcanic glass (Grim and Güven, 1978). Alteration of volcanic ash takes place because the volcanic glass is unstable material and converts to smectite, zeolite and silica polymorphs, releasing metal ions through hydrolysis (Çiftlikli et al., 2013). At the same time, the ash, which covered the bentonitized ash of Zarloukh, was welded, consolidated, and lithified as tuff bed to be covered with time by the recent sediments as overburden. The solid well compacted, very light weighed tuff show many bedding/jointing planes along which bentonitization has also taken place aided by the water infiltrated into these planes of weaknesses which are 10–12 cm thick (Figures 3, 4a). Up to four, such thin bentonite horizons have been found within a 3.2-m-thick tuff in the studied sections (Figure 3). The exposed tuff bed surfaces and joint/fracture planes are stained by recent algae and fungi looking like black organic rich spots (Figure 4b). The similarity of chondrite-normalized REEs distribution patterns for the Zarloukh bentonite and tuff and the Hemrin Basalt, all showing enrichment and negative slope for LREEs relative to the flat-lying HREEs (Figure 7b), is strong evidence for the same origin of the three rock types. This, in turn, suggests that the volcanic eruption in the area was the source of the volcanic ash, which deposited and produced the volcanic tuff and, at the same time, the succeeded lava flow, which created the Hemrin Basalt; the deposited volcanic ash altered in lakes containing very

shallow water, producing the bentonite, which was covered and preserved by the overlying tuff bed.

6. Conclusion

1. The high purity Zarloukh bentonite consists predominantly of montmorillonite with trace to negligible amounts of kaolinite, illite, quartz, dolomite, gypsum, zircon, biotite, and opaques.

2. The Zarloukh deposit consists of bentonite capped by tuff.

3. The Zarloukh bentonite deposit has been formed by the alteration (devitrification-hydration-crystallization) of the volcanic tuff, which was deposited in shallow depressions at the surficial eroded surface of the Muqdadiya Formation.

4. The depressions filled by the flat-lying deposits of bentonite and tuff are remnant of lakes/swamps with shallow water content during the deposition of volcanic ash.

5. The Zarloukh bentonite and tuff and the nearby Hemrin Basalt fall in the field of basaltic andesite–andesites and the high-K calc-alkaline basalt and shoshonite in the Th–Co and the Th/Yb–Ta/Yb diagrams, indicating their common origin.

6. The studied ZBT deposit and the other similar deposits as well as the Hemrin Basalt are of the same origin, formed by a volcanic eruption in the area during the Quaternary period.

7. The studied bentonite compared to its precursor tuff show differences in the concentrations of Ca, Mg, Na, K, Sc, Zr, Hf, Th, La, and Ce because of the bentonitization process of the volcanic ash.

8. The general similarity of the chondrite-normalized REEs distribution pattern for the Zarloukh bentonite and tuff and the Hemrin Basalt with an enrichment and negative slope of LREEs relative to the almost flat-lying HRREs strongly indicates the same origin for all three rock types.

Acknowledgments

The author is thankful to the authorities and technical staff of the Nuclear Research Institute, and the Directorate General of minerals and Mining (Geological Survey of Iraq), Baghdad, Iraq, for their help in analyzing the rock samples. This research did not receive any specific grant from funding agencies in the public, commercial, or not-for-profit sectors.

References

Abdioğlu E, Arslan M, Kolayli H, Kadir S (2004). Mineralogical and geochemical characteristics of the Tirebolu (Giresun) bentonite deposits, NE Turkey. Geochimica et Cosmochimica Acta 68 (11): A416–A416.

Abdioğlu E, Arslan M (2005). Mineralogy, geochemistry and genesis of bentonites of the Ordu area, NE Turkey. Clay Minerals 40: 131–151.

Al-Bassam KS (2012). Mineral deposits and occurrences of the low folded zone. Iraqi Bulletin of Geology and Mining, Special Issue, No.5: Geology of the Low Folded Zone, pp. 159–188.

Al-Hassan MES, Al-Zaidi AH (2012). Sedimentation and facies analysis of volcaniclastic unit within Maqdadia Formation, Injana area, southern Hemrin, NE Iraq. Iraqi Journal of Science 53 (4): 832–841.

Al-Maini J (1975). Preliminary geological report on Emgarin and Tayawi bentonite deposits. GEOSURV Internal Report No. 697.

Al-Naqib KM (1960). Geology of southern area of Kirkuk Liwa, Iraq. Tech. Publ. of IPC, 50p.

Al-Naqib KM (1967). Geology of the Arabian Peninsula: Southwestern Iraq. United States Department of the Interior, Geological Survey, Geology, 54 pages.

Arslan M, Abdioğlu E, Kadir S (2010). Mineralogy, geochemistry, and origin of bentonite in Upper Cretaceous pyroclastic units of the Tirebolu area, Giresun, northeast Turkey. Clays and Clay Minerals 58 (1): 120–141.

Barwary AM, Slewa NA (1991). The Geology of Samarra quadrangleNI-38-6, Scale 1: 250,000. GEOSURV, Baghdad, Iraq.

Basi MA (1973). Geology of Injana area. Hemrin South. M.Sc. thesis. Baghdad University, Baghdad, 127p.

Basi MA, Jassim SZ (1974). Baked and fused Miocene sediments from Injana area, Hemrin South, Iraq. Journal of the Geological Society of Iraq 7: 1–14.

Biscaye PE (1965). Mineralogy and sedimentation of recent deep-sea clay in the Atlantic Ocean and Adjacent seas and oceans. Geological Society of America Bulletin 76: 803–832.

Brown G (1961). The X-ray Identification and Crystal Structures of Clay Minerals. Mineralogical Society (Clay Minerals Group), London, 543 pp.

Carroll D (1970). Clay minerals: A guide to their X Ray identification. Geol. Soc. Am. Sp. Paper 126, Colorado 80p.

Carver RE (1971). Procedures in sedimentary petrography. New York, Wiley-Interscience, 458 p.

Christidis GE, Huff WD (2009). Geological aspects and genesis of bentonites. Elements 5: 93–98.

Çiflikli M, Çiftçi E, Bayhan H (2013). Alteration of glassy volcanic rocks to Na and Ca-smectites in the Neogene basin of Manisa, western Anatolia, Turkey. Clay Minerals 48: 513–527.

Çoban F, Ece OI (1999). Fe^{3+} rich montmorillonite-beidellite series in Ayvacık bentonite deposit, Biga Peninsula, Northwest Turkey. Clays and Clay Minerals 47 (2): 165–173.

El-Khafaji SJR (1989). Rare-Earth Elements Geochemistry of the Industrial Clay Deposits in Iraq. Baghdad University, Baghdad, M.Sc. thesis, 146p.

Elliott WC, Wampler JM, Kadir S, Külah T, Hewitt KC et al. (2020). K–Ar age constraints on the sources of K minerals in bentonites of the Ankara-Çankırı Basin, Central Anatolia, Turkey. International Journal of Earth Sciences 109 (7): 2353–2367.

Fatahi SH, Calagari AA, Abedini A, Bagheri H (2015). Geochemical aspects of Chahreeseh bentonite deposit, northeast of Isfahan, Central Iran Structural Zone. Scientific Quarterly Journal, Geosciences 24 (95): 287–296 (In Persian with English abstract).

Fatahi S, Mackizadeh M, Khani N, Bayat S (2020). Mineralogy, geochemistry and genesis of Mollaahmad Pass bentonite deposit, Naein, Isfahan Province, Iran. Acta Geodynamica et Geomaterialia. 17 (1): 61–87. doi: 10.13168/AGG.2020.0005

Folk RL (1974). Petrology of sedimentary rocks. Austin, TX: Hamphill, 159p.

Gipson M (1966). A study of the relations of depth, porosity, and clay mineral orientation in Pennsylvanian shales. Journal of Sedimentary Research 36 (4): 888–903.

Grim RE, Güven N (1978). Bentonites: Geology, Mineralogy, Properties and Uses. Elsevier, Amsterdam, pp. 13–137.

Hastie AR, Kerr AC, Pearce JA, Mitchell SF (2007). Classification of altered Volcanic Island Arc Rocks using immobile trace elements: development of the Th-Co discrimination diagram. Journal of Petrology 48: 2341–2357.

Kadir S, Erman H, Erkoyun H (2011). Mineralogical and geochemical characteristics and genesis of hydrothermal kaolinite deposits within Neogene volcanites, Kütahya (western Anatolia), Turkey. Clays and Clay Minerals 59 (3): 250–276.

Kadir S, Külah T, Erkoyun H, Christidis GE, Arslanyan R (2019). Geology, mineralogy, geochemistry, and genesis of bentonite deposits in Miocene volcano–sedimentary units of the Balikesir region, western Anatolia, Turkey. Clays and Clay Minerals 67 (5): 371–398.

Kadir S, Külah T, Erkoyun H, Uyanık NÖ, Eren M et al. (2021). Mineralogy, geochemistry, and genesis of bentonites in Upper Cretaceous pyroclastics of the Bereketli member of the Reşadiye Formation, Reşadiye (Tokat), Turkey. Applied Clay Science 204: 106024.

Karakaş Z, Kadir S (2000). Devitrification of volcanic glasses in Konya volcanic units, Turkey. Turkish Journal of Earth Science 9 (1): 39–46.

Karakaya MC, Karakaya N, Kupeli S (2011). Mineralogical and geochemical properties of the Na – and Ca- bentonite of Ordu (NE Turkey). Clay and Clay Minerals 59: 75–94.

Kettanah YA, Abdulrahman AS, Ismail SA, MacDonald DJ, Al Humadi H (2021). Petrography, mineralogy, and geochemistry of the Hemrin Basalt, Northern Iraq: Implications for petrogenesis and geotectonics. Lithos 390–391 (5–6): 106109.

Khatami SSH, Mackizadeh MA, Shamsabadi H (2012). Study of volcaniclastic deposits and formation style of bentonite mine of Chahriseh Abgarm anticline (northeast of Isfahan). Journal of Geotechnical Geology (Applied Geology) 8 (3): 215–224.

Koutsopoulou E, Christidis GE, Marantos I (2016). Mineralogy, geochemistry, and physical properties of bentonites from the western Thrace Region and the islands of Samos and Chios, east Aegean, Greece. Clay Minerals 51: 563–588.

Kukal Z, Al-Jassim J (1971). Sedimentology of Pliocene molasse sediments of the Mesopotamian geosyncline. Sedimentary Geology 5 (1): 57–81.

Külah T, Erkoyun H, Elliott WC (2017). Mineralogy, geochemistry, and genesis of bentonites in Miocene volcanic-sedimentary units of the Ankara-Çankiri basin, central Anatolia, Turkey. Clays and Clay Minerals 65 (2): 64–91.

Malek-Mahmoodi F, Khalili M, Mirlohi A (2013). The origin of the Bentonite deposits of Tashtab Mountains (Central Iran): Geological, Geochemical, and Stable Isotope evidences. The Journal of Geopersia 3 (2): 73–86.

Modabberi S, Namayandeh A, Setti M, Lopez-Galindo A (2019). Genesis of the Eastern Iranian bentonite deposits. Applied Clay Science 168: 56–67.

Mohammed IQ (2019). Bentonite and smectite-rich shale deposits of Iraq: The Geology and Economic Potential of Mineral Deposits and Occurrences of Iraq, Iraqi Bulletin of Geology and Mining Special Issue 8: 175–202.

Nakhaei M, Mohammadi SS, Rasa I, Samiee S (2019). Study of mineralogy, geochemistry and elemental behavior in the process of bentonites formation in Sarbisheh area (South Khorasan, east of Iran). Iranian Society of Crystallography and Mineralogy 27 (1): 207–220.

Pearce JA (1983). Role of sub-continental lithosphere in magma genesis at active margins. In: Hawkesworth CJ, Norry MJ (Eds.), Continental Basalts and Mantle Xenoliths. Shiva Publishers, Nantwich, UK, pp. 230–249.

Sissakian V, Fouad SF (2012). Geological Map of Iraq, 1:1 000 000 Scale Series, Geological Map Publication of GEOSURV, Iraq.

Taylor SR, McLennan SM (1985). The Continental Crust: Its composition and evolution: An examination of the geological record preserved in sedimentary rocks. Oxford, UK: Blackwell 328 pp.

Thorez J (1976). Practical identification of clay minerals: A handbook for teachers and students in clay mineralogy. Editions G. Lelotte, 90 pp.

van Bellen RC, Dunnington HV, Wetzel, Morton DM (1959). Lexique Stratigraphique International. Asie, Fase, 10a, Iraq. Paris: CNRS, 1-333.

Wilson M, Bianchini G (1999). Tertiary-Quaternary magmatism within the Mediterranean and surrounding regions. Geological Society Special Publication 156: 141–168.

Yalçın H, Gümüşer G (2000). Mineralogical and geochemical characteristics of Late Cretaceous bentonite deposits of the Kelkit Valley Region, Northern Turkey. Clay Minerals 35: 807–825.

Yıldız A, Dumlupunar I (2009). Mineralogy and geochemical affinities of bentonites from Kapıkaya (Eskişehir, western Turkey). Clay Minerals 44 (3): 339–360.

Yıldız A, Kuşcu M (2004). Origin of the Başoren (Kutahya, W Turkey) bentonite deposits. Clay Minerals 39: 219–231.

Yıldız A, Kuşcu M (2007). Mineralogy, chemistry and physical properties of bentonites from Başoren, Kutahya, W Anatolia, Turkey. Clay Minerals 42: 399–414.

Zainal YM (1977). Mineralogy, geochemistry, and origin of some Tertiary bentonites in Iraq. Ph.D. Thesis. Sheffield University, UK.

Zainal YM. Jargees S (1972). Geological report on Qara-Tappa bentonite. GEOSURV, Internal Report No. 546.

Zainal YM, Jargees S (1973). Preliminary geological report on Zarloukh montmorillonite clay (bentonite) prospect. GEOSURV, Internal Report No. 578.